Structural Engineering and Mechanics, Vol. 10, No. 5 (2000) 451-462
DOI: http://dx.doi.org/10.12989/sem.2000.10.5.451

Use of the differential quadrature method for the buckling analysis of cylindrical shell panels

D. Redekop† and E. Makhoul‡

Department of Mechanical Engineering, University of Ottawa, Ottawa, Ontario, Canada K1N 6N5

Abstract. Buckling loads are determined for thin isotropic circular cylindrical shell panels subject to radial pressure using the new differential quadrature method. The Budiansky stability theory serves as the basis of the analysis. For this problem involving four boundary lines a two-dimensional approach is used, and a detailed convergence study is carried out to determine the appropriate analysis parameters for the method. Numerical results are determined for a total of twelve cylindrical shell panel cases for a number of different boundary support conditions. The results are compared with analytical and finite element method results. Conclusions are drawn about the technical significance of the results and the solution process.

Key words: Stability analysis; cylindrical panels; differential quadrature method.

1. Introduction

The stability analysis of shell structures continuous to be a very active area of engineering research (Vandepitte 1999, Yamaki 1984). Among the geometries of interest are cylindrical shell panels which exhibit very favorable strength-over-weight ratios in light-weight structures. They are used in such different applications as space and ground vehicles, marine structures, turbo-machinery blades, and vaulted shell roofs. Due to their thinness though, they are susceptible to structural instability.

The literature on cylindrical shell panels under pressure loading is relatively sparse. Recent studies includes a buckling analysis based on the Flügge theory (Makhoul 1999, 2000), a simplified dynamic buckling analysis (Kounadis and Sophianopoulos 1996), a dynamic response analysis (Redekop and Azar 1991), and a non-linear buckling analysis (Yamada and Croll 1989). The latter work is a comprehensive theoretical study of the topic. To date no detailed study has appeared providing comparison of theoretical results for panel buckling with results from a numerical or experimental study.

In this paper the new differential quadrature method (DQM) in its two-dimensional form is used to provide a theoretical solution to the instability problem of an isotropic circular cylindrical shell panel subject to radial pressure. The linearized thin shell stability theory of Budiansky (1968) serves as the basis of the analysis. A detailed study is conducted of the convergence properties of the DQM, and results are presented covering a wide range of shell geometric parameters and practical

† Professor
‡ M.A. Sc.

boundary conditions. Results obtained from the DQM are compared with those from a pure analytical solution and a finite element method (FEM) solution.

2. Geometry and boundary conditions

The panel under consideration has a length of L, and a width in plan of H (Fig. 1). The thickness is h and the maximum rise above the base plane is f. The shell radius R is given by $H^2/(8f)+f/2$, and the subtended angle is given by $\theta_o=2arcsin[H/(2R)]$. The cylindrical shell axis x is parallel to the shell length while the geodetic coordinate y follows the shell circumference. Displacements u, v are in-plane, while w is perpendicular to the shell surface, positive inwards. A uniform inward radial pressure of p is assumed to act on the mid-surface.

In the DQM analysis three types of support are considered for the panel edges; roller (R), pinned (S), and clamped (C). The boundary conditions on the $x=cnst$ edges for these three types are given respectively by

$$\begin{aligned} &u = 0;\ v = 0;\ w = 0;\ M_x = 0 \\ &N_x = 0;\ v = 0;\ w = 0;\ M_x = 0 \\ &u = 0;\ v = 0;\ w = 0;\ w_{,x} = 0 \end{aligned} \tag{1}$$

Similar conditions can be written for the $y = cnst$ edges.

3. Budiansky shell stability theory

To determine the buckling loads for the panel the Budiansky linearized shell stability theory (Budiansky 1968) is employed. The governing equations, written in terms of coordinates $\xi = x/R$ and $\theta = y/R$, are given by

$$[L]\{U\} + \lambda[\hat{L}]\{U\} = \{Q\} \tag{2}$$

where

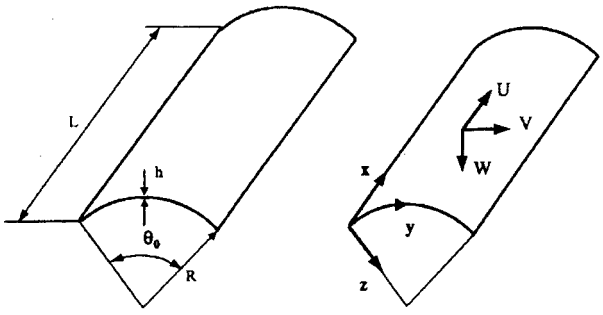

Fig. 1 Geometry

$$[L]=\begin{bmatrix} \frac{\partial^2}{\partial\xi^2}+\frac{1-\nu}{2}\left(1+\frac{k}{4}\right)\frac{\partial^2}{\partial\theta^2} & \left(\frac{1+\nu}{2}-\frac{1-\nu}{2}\frac{3k}{4}\right)\frac{\partial^2}{\partial\xi\partial\theta} & \nu\frac{\partial}{\partial\xi}+\frac{1-\nu}{2}k\frac{\partial^3}{\partial\xi\partial\theta^2} \\ \left(\frac{1+\nu}{2}-\frac{1-\nu}{2}\frac{3k}{4}\right)\frac{\partial^2}{\partial\xi\partial\theta} & \frac{1-\nu}{2}\left(1+\frac{9k}{4}\right)\frac{\partial^2}{\partial\xi^2}+(1+k)\frac{\partial^2}{\partial\theta^2} & \frac{\partial}{\partial\theta}-\frac{3-\nu}{2}k\frac{\partial^3}{\partial\xi^2\partial\theta}-k\frac{\partial^3}{\partial\theta^3} \\ \nu\frac{\partial}{\partial\xi}+\frac{1-\nu}{2}k\frac{\partial^3}{\partial\xi\partial\theta^2} & \frac{\partial}{\partial\theta}-\frac{3-\nu}{2}k\frac{\partial^3}{\partial\xi^2\partial\theta}-k\frac{\partial^3}{\partial\theta^3} & 1+k\left(\frac{\partial^4}{\partial\xi^4}+2\frac{\partial^4}{\partial\xi^2\partial\theta^2}+\frac{\partial^4}{\partial\theta^4}\right) \end{bmatrix} \tag{3}$$

and

$$[\hat{L}]=\begin{bmatrix} n_\xi\frac{\partial^2}{\partial\xi^2}+n_\theta\frac{\partial^2}{\partial\theta^2}+2n_{\xi\theta}\frac{\partial^2}{\partial\xi\partial\theta} & 0 & -Rp\frac{\partial}{\partial\xi} \\ 0 & n_\xi\frac{\partial^2}{\partial\xi^2}+n_\theta\left(\frac{\partial^2}{\partial\theta^2}-1\right)+2n_{\xi\theta}\frac{\partial^2}{\partial\xi\partial\theta}+Rp & 2n_\theta\frac{\partial}{\partial\theta}+2n_{\xi\theta}\frac{\partial}{\partial\xi}-Rp\frac{\partial}{\partial\theta} \\ -Rp\frac{\partial}{\partial\xi} & 2n_\theta\frac{\partial}{\partial\theta}+2n_{\xi\theta}\frac{\partial}{\partial\xi}-Rp\frac{\partial}{\partial\theta} & -n_\xi\frac{\partial^2}{\partial\xi^2}+n_\theta\left(-\frac{\partial^2}{\partial\theta^2}+1\right)-2n_{\xi\theta}\frac{\partial^2}{\partial\xi\partial\theta}-Rp \end{bmatrix} \tag{4}$$

The vector of displacements $\{U\}$ represents $\{u\ v\ w\}^t$, while the vector of loads $\{Q\}$ is given by $\{0\ 0\ R^2p\}^t$. The quantities n_ξ, n_θ, and $n_{\xi\theta}$ represent respectively the axial, circumferential, and in-plane shear membrane stress resultants in the shell just prior to buckling. The geometric factor k is defined as $k=\frac{1}{12}\left(\frac{h}{R}\right)^2$, ν is the Poisson's ratio, and λ is the buckling load parameter.

The governing equations must be solved subject to the boundary conditions. For each of the four edges there are four boundary conditions. Resultants appearing in the boundary conditions can be expressed in terms of the displacements using relations given by Budiansky. The procedure developed allows for the specification of any of the three support types (R, S, C) on any of the four edges. The conversion of the governing equations and the boundary conditions into a form suitable for the DQM is discussed in the following section.

4. Differential quadrature method

The basis of the DQM (Bert and Malik 1996) is the representation in the domain of the derivatives of a function by a weighted sum of trial function values. Thus for a function of one variable $f(x)$ the derivatives are taken as

$$\left.\frac{d^r f(x)}{dx^r}\right|_{x_i}=\sum_{k=1}^{N_1}A_{ik}^{(r)}f(x_k) \tag{5}$$

while for a function of two variables $g(x, y)$ they are taken as

$$\left.\frac{\partial^{(r+s)} g(x, y)}{\partial x^r \partial y^s}\right|_{x_i, y_j} = \sum_{k=1}^{N_I} A_{ik}^{(r)} \sum_{l=1}^{N_J} B_{jl}^{(s)} g(x_k, y_l) \tag{6}$$

Here the $A_{ik}^{(r)}$ are the weighting coefficients of the r-th order derivative at the i-th sampling point in the x direction, and N_I is the number of sampling points in the x direction. The $B_{jl}^{(s)}$ used for the y direction are similarly defined.

Polynomial trial functions are selected in this study, i.e. $f(\xi)=1, \xi, \xi^2, \cdots, \xi^{N_I-1}$ for the x direction. For these functions explicit formulas for the weighting coefficients are available (Bert and Malik 1996). For the first order derivative the formulas are

$$A_{ij}^{(1)}=\frac{\pi(\xi_i)}{(\xi_i-\xi_j)\pi(\xi_j)}; \quad i, j=1, 2, \cdots, N_I; \; i \neq j$$

$$\pi(\xi_i)=\prod_{j=1}^{N_I}(\xi_i-\xi_j); \quad i \neq j \tag{7}$$

while for the higher order derivatives the formulas are

$$A_{ij}^{(r)}=r\left[A_{ii}^{(r-1)} A_{ij}^{(1)}-\frac{A_{ij}^{(r-1)}}{\xi_i-\xi_j}\right]; \quad i, j=1, 2, \cdots, N_I; \; i \neq j; \; 2 \leq r \leq (N_I-1)$$

$$A_{ij}^{(r)}=A_{ii}^{(r)}=-\sum_{k=1}^{N_I} A_{ik}^{(r)}; \quad i=1, 2, \ldots, N_I; \; i \neq k; \; 1 \leq r \leq (N_I-1) \tag{8}$$

The Chebyshev-Gauss-Lobatto spacing (Bert and Malik 1996) is used for the positioning of the sampling points. In this scheme the coordinates are taken as $\xi_i=\alpha_i(L/R)$ where the α_i are given by

$$\alpha_1=0; \quad \alpha_2=\delta; \quad \alpha_{N_I-1}=1-\delta; \quad \alpha_{N_I}=1$$

$$\alpha_i=\frac{1-\cos\dfrac{\pi(i-2)}{N_I-3}}{2}; \quad 2<i<(N_I-1) \tag{9}$$

At each sampling point either the DQM analogue of a governing equation for the domain or a condition for the boundary support is represented. For each boundary point there are four conditions, while for each domain point there are only three governing equations. It is necessary to enforce one of the boundary conditions at an interior point. This point, a 'δ point', is taken a short distance ($\delta=10^{-4}$ or $\delta=10^{-5}$ on a unit domain) from the boundary point. Corner points of the panel apparently require special treatment. In the present study these points are simply assigned to the straight edges.

For the representation of derivatives in the circumferential direction a similar system is used, namely a polynomial expansion and a Chebyshev-Gauss-Lobatto spacing of sampling points. The weighting coefficients are now represented by the symbols $B_{ij}^{(r)}$ and the number of sampling points by N_J.

Use in the governing Eqs. (2) of the operators (3-4) and the quadrature rules for the derivatives (5-8) leads to the transformed DQM domain equations. The resulting equations have the form

$$\sum A_{ij}^{(2)}U_{jh}+\frac{1-\nu}{2}\left(1+\frac{k}{4}\right)\sum B_{hl}^{(2)}U_{il}+\left(\frac{1+\nu}{2}-\frac{1-\nu}{2}\frac{3k}{4}\right)\sum A_{hl}^{(1)}\sum B_{ij}^{(1)}V_{jl}$$
$$+\nu\sum A_{ij}^{(1)}W_{jh}+\frac{1-\nu}{2}k\sum A_{hl}^{(1)}\sum B_{ij}^{(2)}W_{jl}+\lambda[n_{\xi}\sum A_{ij}^{(2)}U_{jh}$$
$$+n_{\theta}\sum B_{hl}^{(2)}U_{il}+2n_{\xi\theta}\sum A_{hl}^{(1)}\sum B_{ij}^{(1)}U_{jl}-Rp\sum A_{ij}^{(1)}W_{jh}]=0$$

$$\left(\frac{1+\nu}{2}-\frac{1-\nu}{2}\frac{3k}{4}\right)\sum A_{hl}^{(1)}\sum B_{ij}^{(1)}U_{jl}+\frac{1-\nu}{2}\left(1+\frac{9k}{4}\right)\sum A_{ij}^{(2)}V_{jh}$$
$$+(1+k)\sum B_{hl}^{(2)}V_{il}-(k\sum B_{hl}^{(3)}-\sum B_{hl}^{(1)})W_{il}-\frac{3-\nu}{2}k\sum A_{hl}^{(2)}\sum B_{ij}^{(1)}W_{jl}$$
$$+\lambda[n_{\xi}\sum A_{ij}^{(2)}V_{jh}+n_{\theta}(\sum B_{hl}^{(2)}V_{il}-V_{ih})+2n_{\xi\theta}\sum A_{hl}^{(1)}\sum B_{ij}^{(1)}V_{jl}+RpV_{ih}$$
$$+(2n_{\theta}-Rp)\sum B_{hl}^{(1)}W_{il}+2n_{\xi\theta}\sum A_{ij}^{(1)}W_{jh}]=0$$

$$\nu\sum A_{ij}^{(1)}U_{jh}+\frac{1-\nu}{2}k\sum A_{hl}^{(1)}\sum B_{ij}^{(2)}U_{jl}-(k\sum B_{hl}^{(3)}-\sum B_{hl}^{(1)})V_{il}$$
$$-\frac{3-\nu}{2}k\sum A_{hl}^{(2)}\sum B_{ij}^{(1)}V_{jl}+k(\sum A_{ij}^{(4)}W_{jh}+2\sum A_{hl}^{(2)}\sum B_{ij}^{(2)}W_{jl}+\sum B_{hl}^{(4)}W_{il})$$
$$+W_{ih}+\lambda[-Rp\sum A_{ij}^{(1)}U_{jh}+(2n_{\theta}-Rp)\sum B_{hl}^{(1)}V_{il}+2n_{\xi\theta}\sum A_{ij}^{(1)}V_{jh}$$
$$-n_{\xi}\sum A_{ij}^{(2)}W_{jh}+n_{\theta}(W_{ih}-\sum B_{hl}^{(2)}W_{il})-2n_{\xi\theta}\sum A_{hl}^{(1)}\sum B_{ij}^{(1)}W_{jl}-RpW_{ih}]=R^2p \qquad (10)$$

where the U_{ij}, etc. are unknown displacements at the sampling points. The expressions involving the boundary conditions on the edges may similarly be transformed.

The assembly of the domain and boundary equations yields a matrix equation of the form

$$[K_s]\{\Delta\}+\lambda[K_g]\{\Delta\}=\{q\}$$

The stiffness and geometric matrices $[K_s]$ and $[K_g]$ stem initially from the $[L]$ and $[\hat{L}]$ operators of the governing equations, and are of size $3\times N_x\times N_y$. Replacement of the domain equations at the boundary points by the support conditions brings these matrices to their final form. The vector $\{\Delta\}$ contains the displacements at all the sampling points while the vector q the applied pressure at the sampling points.

Eq. (11) may be used to solve the problems of stress and buckling analysis. For the stress analysis problem the parameter λ is zero, while for the buckling analysis problem the vector $\{q\}$ is zero. For the buckling problem the smallest eigenvalue, $\lambda_{\min}$, corresponding to the minimum critical pressure, may be found using standard eigenvalue extraction routines. The theory presented in the preceding was programmed in a MATLAB code labelled panbud.m. Results from this program are given in the following.

5. Finite element method

The commercial FEM program NE/NASTRAN (NE/Nastran 1998) was used to provide a

comprehensive verification of the DQM theoretical results. A flat four-noded twenty-four degree-of-freedom shell element is available in this program for the solution of shell stress analysis and stability problems.

The entire shell panel was modelled in each case, as buckling modes are not necessarily symmetric. Clamped, simply supported, roller, and free conditions on the boundaries were easily modelled as required. Results were found for several mesh sizes to indicate the convergence of the solution. For the final analysis a mesh of 40×40 elements was employed.

6. Results

Sample numerical results are presented in this section for steel panels having a Young's modulus of 200,000 MPa, and a Poisson's ratio of 0.3. Results are obtained for twelve panel cases, described in Table 1. The θ_o in this table gives the subtended angle of the panels. Panels 1-4 are short, panels 5-8 are square in plan, and panels 9-12 are long. In each of these three groups the first two panels are relatively thick (R/t=100), while the last two are thin (R/t=200). Two cases of panel rise are considered; the first is a low rise (0.1 of the panel width), and the last is a moderate rise (0.2 of the panel width).

A careful consideration was made in the choice of the mesh grid for the DQM analysis. For convenience an equal number of sampling points ($N_I = N_J = N_g$) was taken for the axial and circumferential directions for all twelve cases (Fig. 2). For this choice the aspect ratio of sampling point spacing in the two directions for the twelve panel cases varied from about 1:2 to 2:1, which represents a fairly severe test of the method. For the FEM an equal number of elements was taken in the two directions, leading to element aspect ratios for the twelve cases which were well within accepted limits.

Results for panels with RRRR supports on all four edges are given in Table 2. The factorized critical buckling pressure is given for each of the twelve cases from four different analyses. Results obtained from the current panbud.m DQM program are given in the second column. Results

Table 1 Description of panel cases

Case	*L/H*	*R/t*	*f/H*	θ_o (deg)
1	0.5	100	0.1	45.2397
2	0.5	100	0.2	87.2056
3	0.5	200	0.1	45.2397
4	0.5	200	0.2	87.2056
5	1.0	100	0.1	45.2397
6	1.0	100	0.2	87.2056
7	1.0	200	0.1	45.2397
8	1.0	200	0.2	87.2056
9	2.0	100	0.1	45.2397
10	2.0	100	0.2	87.2056
11	2.0	200	0.1	45.2397
12	2.0	200	0.2	87.2056

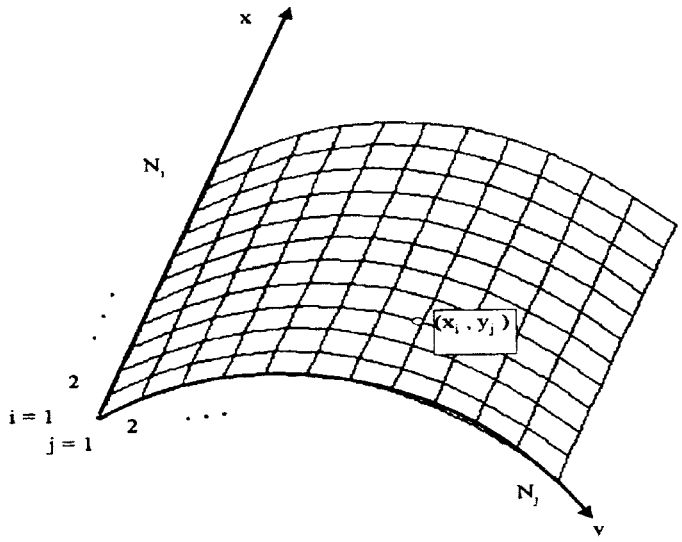

Fig. 2 DQM mesh

Table 2 Results for roller supported edges (RRRR)

	Critical pressure p/E ($\times 10^{-4}$)			
Case	DQM	Makhoul	Exact	FEM
1	.3501	.3502	.3530	.3315
2	.1624	.1739	.1637	.1621
3	.0544	.0548	.0548	.0538
4	.0271	.0273	.0299	.0274
5	.1438	.1428	.1618	.1410
6	.0769	.0819	.0788	.0783
7	.0243	.0245	.0241	.0242
8	.0124	.0127	.0126	.0126
9	.0714	.0692	.0711	.0711
10	.0399	.0361	.0395	.0413
11	.0105	.0119	.0112	.0106
12	.0060	.0063	.0060	.0061

obtained from a program pann2k.f90 which is based on a development by Makhoul (2000) are given in the third column. The approach used by Makhoul closely resembled that of the current study, but a simple membrane state was assumed to preside prior to buckling, and the Flügge shell theory was used instead of the Budiansky theory. Closed form (exact) analytical results (Makhoul and Redekop 1999) obtained from a program flug.m are given in the fourth column, and in Fig. 3. In this exact solution the trigonometric terms selected for each coordinate direction satisfied exactly the governing equations and the boundary conditions. Such an exact solution is possible only with the RRRR support condition. Finally results obtained from the FEM program NE-NASTRAN are given in the fifth column.

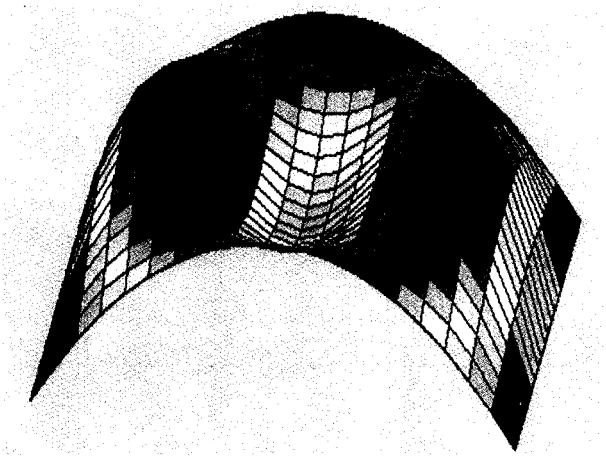

Fig. 3 Exact mode for Case 9 - RRRR

The results confirm a number of observations that have been made previously about cylindrical panel buckling. Firstly, the critical pressure decreases as the shell length is increased. This is according to expectation, as stiffeners serve to increase resistance to buckling as they create shorter effective shell lengths. Secondly, the critical pressure decreases as the thickness is decreased. Clearly decreasing the thickness decreases the panel stiffness. Thirdly, the critical pressure decreases as the panel rise is increased. Panel buckling is due to membrane action, and increase of shell curvature increases the level of membrane stress.

There is generally good agreement in the results from the various theories and methods for all twelve cases. The DQM results given in the second column are derived from the Budiansky buckling equations in which the prebuckling membrane stresses appear directly, having been determined from a prior analysis in which the appropriate boundary conditions were satisfied. The results from the third and fourth columns are derived from the Flügge buckling equations, in which the surface loading terms appear directly, and no prior analysis for prebuckling membrane stresses has been made. The Flügge analytical results may be considered to give the exact solution, and it is seen that the current DQM and FEM results generally show very close agreement with these for all twelve cases, with a maximum error of about 5%.

An indication of the convergence characteristics of the current DQM approach is given in Table 3. The case considered is the first one of Table 1, for which convergence was noted to be slow. The study covers three types of the supports on the four edges; RRRR, SSSS, and CCCC. Results corresponding to different choices of the number of sampling points ($N_g = N_I = N_J$), are given for two values of the boundary δ distance. The terms of the converging series are divided into two groups, corresponding to even and odd choices for N_g. Results from the FEM are also given, together with the size of the FEM mesh (N_e). The largest DQM grid considered was one having 22 sampling points in each direction.

It is seen that for this case convergence is clear only for the RRRR support condition. There is agreement to three figures in the results for the meshes consisting of 15 and 16 sampling points. Furthermore the even and odd series clearly converge to the same value. For the other two support conditions the convergence, although present, is less clear. There is a slight difference in the final even and odd series results (about 2%), and the convergence although rapid initially does not show

Table 3 Convergence of DQM for case 1

	Critical pressure p/E ($\times 10^{-4}$)				
	$\delta=10^{-4}$		$\delta=10^{-5}$		FEM
Ng	odd	even	odd	even	(Ne)
RRRR					
9,10	.430254	.381292	.431458	.380973	
11,12	.362658	.350487	.362845	.350436	
13,14	.352468	.349518	.352465	.349506	
15,16	.350387	.350103	.350358	.350085	.3315(40)
SSSS					
9,10	.447804	.403645	.448868	.404122	
11,12	.371272	.392881	.373174	.393019	
13,14	.369448	.389792	.371612	.390027	
15,16	.373890	.389386	.376384	.389705	
17,18	.376846	.389678	.379759	.390060	
19,20	.378103	.389754	.381576	.390218	
21,22	.378792	.389822	.382959	.390381	.3722(40)
CCCC					
9,10	.734101	.680874	.735672	.682209	
11,12	.601935	.611352	.603908	.612259	.5824(35)
13,14	.580220	.603233	.583955	.603874	.5813(36)
15,16	.583725	.604203	.587443	.604861	.5801(37)
17,18	.585929	.604767	.590436	.605555	.5790(38)
19,20	.587986	.604907	.593328	.605891	.5779(39)
21,22	.589155	.604829	.595506	.606080	.5768(40)

Table 4 Results for pinned straight edges

	Critical pressure p/E ($\times 10^{-4}$)				
	SSSS		SCSC		SFSF
Case	DQM	FEM	DQM	FEM	FEM
1	.3898	.3722	.5592	.5297	.0560
2	.1917	.1952	.2162	.2178	.0152
3	.0630	.0629	.0757	.0753	.0071
4	.0333	.0345	.0358	.0367	.0019
5	.1991	.1952	.2162	.2112	.0570
6	.1103	.1117	.1147	.1158	.0153
7	.0363	.0363	.0376	.0376	.0072
8	.0191	.0193	.0194	.0196	.0019
9	.1427	.1429	.1448	.1444	.0575
10	.0675	.0691	.0683	.0695	.0154
11	.0208	.0212	.0212	.0214	.0072
12	.0108	.0110	.0110	.0111	.0019

Table 5 Results for clamped straight edges

	Critical pressure p/E ($\times 10^{-4}$)				
	CCCC		CSCS		CFCF
Case	DQM	FEM	DQM	FEM	FEM
1	.6048	.5768	.4146	.3982	.1182
2	.2211	.2241	.1958	.1997	.0326
3	.0784	.0783	.0656	.0656	.0128
4	.0367	.0379	.0341	.0355	.0041
5	.2660	.2605	.2507	.2464	.1197
6	.1200	.1214	.1164	.1180	.0328
7	.0423	.0424	.0405	.0407	.0149
8	.0202	.0205	.0198	.0215	.0041
9	.1800	.1793	.1761	.1768	.1204
10	.0750	.0775	.0738	.0770	.0330
11	.0276	.0282	.0272	.0279	.0150
12	.0121	.0124	.0119	.0123	.0041

signs of complete stabilization. Thus in any quotation of results there will be a slight difference depending whether the reference is to an odd or even series. The results for a choice of $\delta=10^{-4}$ differ slightly (about 2%) from those for a choice of $\delta=10^{-5}$. Use of a custom eigenvalue extractor that was dedicated to finding the lowest eigenvalue lead to results about 1% different from those given here which were found using the MATLAB built-in eigenvalue extractor. The differences referred to however are small, and can be tolerated in an engineering solution. The results given in Table 2, and subsequently, correspond to a choice of $\delta=10^{-4}$, the use of a maximum of 22 sampling points, and the use of the MATLAB built-in eigenvalue extractor.

Results for problems involving pinned supports on the straight edges are given in Table 4. DQM results are given for the case of pinned and clamped support conditions on the curved edges. FEM results are given for the same types of curved edge support, as well as for 'free supports'. Similar

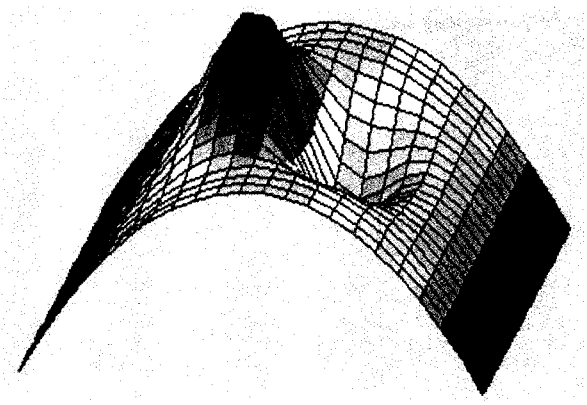

Fig. 4 DQM mode for case 9 - CCCC

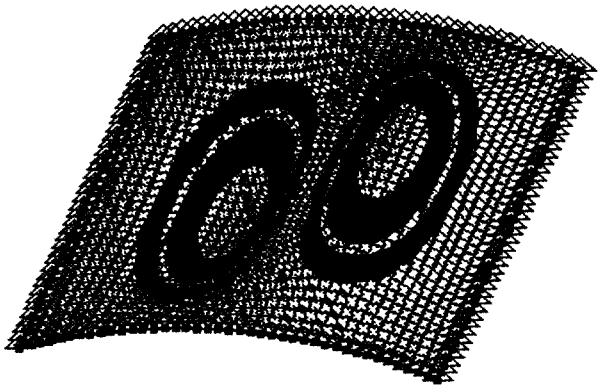

Fig. 5 FEM mode for case 9 - CCCC

sets of results for problems involving clamped straight edges are given in Table 5. Theoretical results for free support conditions are found invariably only with much greater effort than for other conditions. Thus the determination of DQM results for these cases was not considered within the scope of the present study. Finally mode shapes found using the DQM and FEM are given in Figs. 4-5.

The trends mentioned in regard to Table 2 are observed also in Tables 4 and 5. It is noted that the type of boundary support has a significant influence on the critical buckling pressure. In general changing from a pinned to a clamped support significantly increases the buckling pressure. Changing from a pinned to a free support has the opposite effect. Comparing the results from the two methods, it is seen that there is generally very close agreement in critical pressure. Also Figs. 4 and 5 indicate a strong resemblance in the mode shapes. Considering the vast differences in the details of the idealization, and in the determination of the numerical results for the DQM and FEM, the agreement is remarkable.

7. Conclusions

A solution to the buckling problem of an isotropic cylindrical shell panel has been presented. A study of the convergence characteristics of the differential quadrature solution has shown that there is considerable flexibility in the choice of sampling point spacing. As well there is considerable versatility with regard to the boundary conditions. Overall the study shows that results for panel buckling loads obtained from the differential quadrature method agree very closely with results from the finite element method.

Acknowledgement

This study was supported in part by a grant from the Natural Sciences and Engineering Research Council of Canada.

References

Bert, C.W. and Malik, D. (1996), "Free vibration analysis of thin cylindrical shells by the differential quadrature method", *ASME J. Pres. Ves. Techn.*, **118**, 1-12.

Budiansky, B. (1968), "Notes on nonlinear shell theory", *ASME J. Appl. Mech.*, **40**, 393-401.

Flügge, W. (1973), *Stresses in Shells*, 2nd Ed., Springer, Berlin.

Kounadis, A.N. and Sophianopoulos, D.S. (1996), "Nonlinear dynamic buckling of a cylindrical shell panel model", *AIAA J*, **34**, 2421-2428.

Makhoul, E., *Buckling of Thin Circular Cylindrical Shell Panels by the Differential Quadrature Method*, M. A. Sc., Univ. of Ottawa, 2000.

Makhoul, E. and Redekop, D. (1999), "Buckling of cylindrical shell panels using the DQM", *Proc. 1st Int. Conf. on Advances in Struct. Eng. Mech.*, Seoul, **1**, 353-358.

NE/NASTRAN, (1998), *User's Manual*, v. 4.0, Noran Engineering, Inc., Garden Grove, CA.

Redekop, D. and Azar, P. (1991), "Dynamic response of a cylindrical shell panel to explosive loading", *ASME J. Vib. Acoust.*, **113**, 273-278.

Vandepitte, D. (1999), "Confrontation of shell buckling research results with the collapse of a steel water tower", *J. Const. Steel Research*, **49**, 303-314.

Yamada, S. and Croll, J.G.A. (1989), "Buckling behavior of pressure loaded cylindrical panels", *ASCE J. Eng. Mech.*, **115**, 327-344.

Yamaki, N. (1984), *Elastic Stability of Circular Cylindrical Shells*, North Holland, New York.